Supporting Information

Ordered Monolayers of Free Standing Porphyrins on Gold

Franziska L. Otte,[†] Sonja Lemke,[‡] Christian Schütt,[†] Nicolai R. Krekiehn,[‡] Ulrich Jung,[‡] Olaf M. Magnussen*,[‡] Rainer Herges*[†].

[†]Otto-Diels-Institute for Organic Chemistry, Christian-Albrechts-University of Kiel, 24098 Kiel, Germany

[‡]Institute for Experimental and Applied Physics, Christian-Albrechts-University of Kiel, 24098 Kiel, Germany

Table of Contents

S1 Computational Details

S1.1 Optimization of the Dimers of porphyrin-TATA 1 and 2

The optimizations of porphyrin-TATA **1** and **2** (Figure 3 in the main text) were performed at the PBE/SVP-D2 level of density functional theory using Turbomole 6.2[1]. The octyl side chains were replaced by methyl groups to save computational cost. The distance between the dimers was taken from the STM experiment. To include the geometry constraints of the surface, the platforms of each porphyrin-TATA (plane defined by the N atoms) were forced to lie within an imaginary plane. Thus electronic effects of the gold surface are not considered.

S.1.2 Rotational barrier of porphyrin-TATA 1 and 2

To estimate the energy barrier for the rotation of the porphyrin substituent potential energy surface scans of compounds **1** and **2** were performed at the B3LYP[2-4]/6-31G* level of theory using Gaussian 09 Rev. D01[5]. Propyl side chains were used to include the steric effects of the alkyl side chains at the TATA platform with respect to the rotation of the porphyrin. The orientation of the alkyl side chains of the TATA was elucidated in our previous work[6]. The energy surface scans for the rotation of 5-ethinyl(Zn)porphin (**1**) and the 5-ethinyl-5-10-15-triphenyl-(Zn)porphyrin (**2**) substituent around the C-C triple bond are shown in Figure S1. Six maxima were found at the positions where the one of the β-protons (the pyrrol protons of the porphyrin) is in close proximity to an alkyl side chain. The energy barrier for the rotation (0.3 kcal mol^{-1}) is lower than *kT* (0.6 kcal mol^{-1}) which leads us to the conclusion that the Zn-porphin **1** and Zn-porphyrin **2** can rotate freely at room temperature in isolated molecules (intermolecular interactions not included).

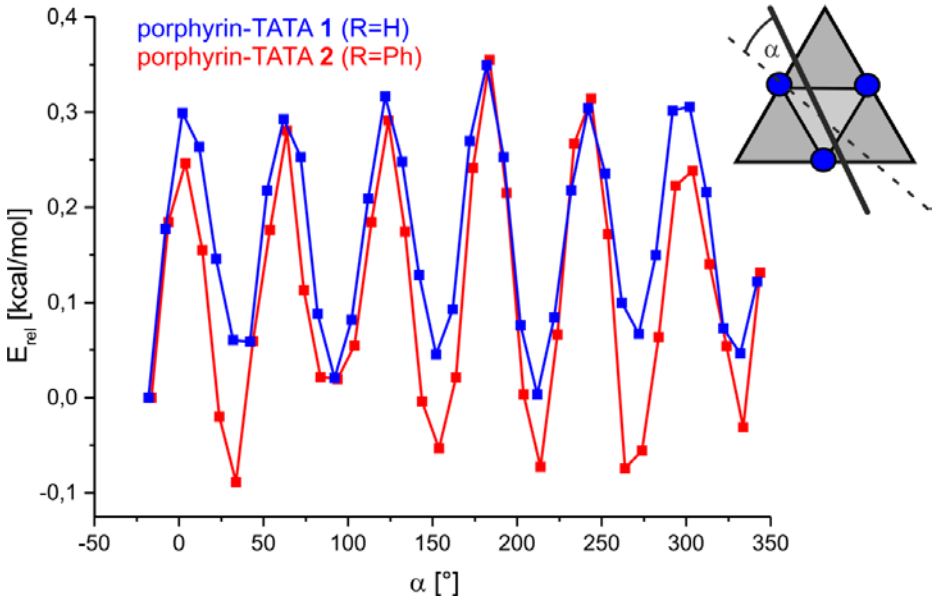

Figure S1 Potential energy surface scan for the rotation of the 5-ethinyl-(Zn)porphin-TATA (**1**) (blue) and 5-ethinyl-5-10-15-triphenyl-(Zn)porphyrin-TATA (**2**) (red). The angle α was increased in steps of 10° and all other geometry parameters were optimized at the B3LYP/6-31G* level of theory. For clarity the TATA platform is represented as a triangle. The blue dots are the TATA nitrogen atoms. The porphyrin is represented as a black bar.

S.1.3 Rotational barrier of the porphyrin-TATA 1 and 2 dimers

To estimate steric interactions between neighboring porphyrin TATA molecules potential energy surface scans of the dimers of porphyrin-TATA **1** and **2** were performed at the B3LYP/6-31G*-D3[7a] level of theory using Gaussian 09 Rev. D01. Optimized structures were used as starting points for potential energy surface scans. Angle β was varied and single point energy calculations were performed. The alkyl side chains were replaced by methyl groups to save computational cost (Figure S2). As expected, the energy barrier for the rotation of **1** is still lower than k*T* (blue line). Therefore porphyrin **1** can rotate freely at room temperature. This is in agreement with an averaged the hexagonal symmetry of the SAM observed by STM. The rotation of porphyrin **2**, however, is sterically hindered due to the *meso* phenyl rings of the porphyrin (red curve). London dispersion interaction between the phenyl groups of neighboring porphyrin-TATA molecules gives rise to a minimum on the rotational hypersurface which is about 4 kcal mol^{-1} lower in energy than two non-interacting molecules. As a result **2** forms the novel double-row structures on the Au(111) surface.

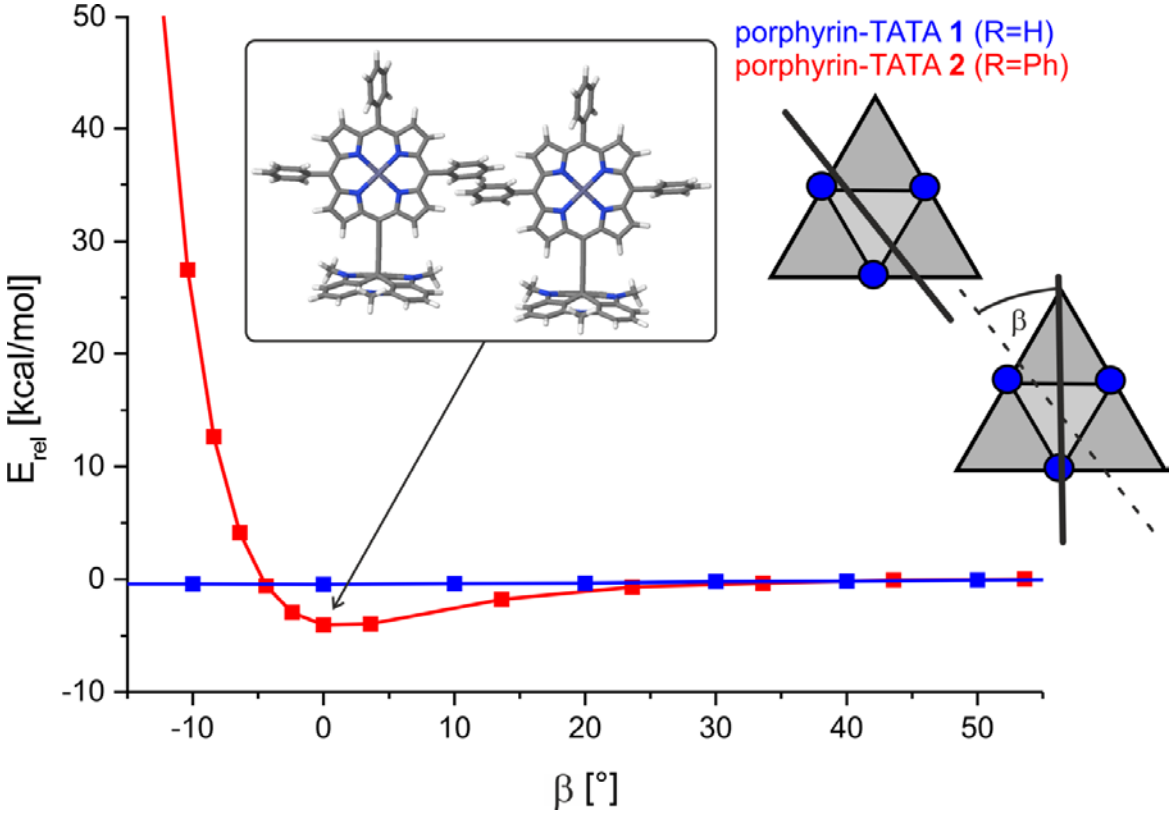

Figure S2 Rigid potential energy surface scan for the rotation of the 5-ethinyl-(Zn)porphin-TATA (**1**) (blue), 5-ethinyl-5-10-15-triphenyl-(Zn)porphyrin-TATA (**2**) (red curve) as a function of angle β at the B3LYP/6-31G*-D3 level of theory. The distances between the molecules are taken from STM. One of the porphyrin-TATA structures (the upper left one in the schematic representation) is frozen with respect to all geometry parameters. Angle β is varied in the other structure. For clarity the TATA platform is represented as a triangle. The blue dots are the platform nitrogen atoms. The porphyrin is represented as a black bar.

S1.4 TDDFT calculations of porphyrin-TATA 2

The TDDFT calculation of porphyin-TATA **2** was performed at the B3LYP/6-31G* level of density functional theory. Note that the wavelengths of the transitions predicted by the TDDFT calculations are systematically 10-30 nm hypsochromic with respect to our experimental UV-VIS spectra which is a known problem at this level of theory.[7b] An excerpt of the corresponding log file is given in section S1.5.

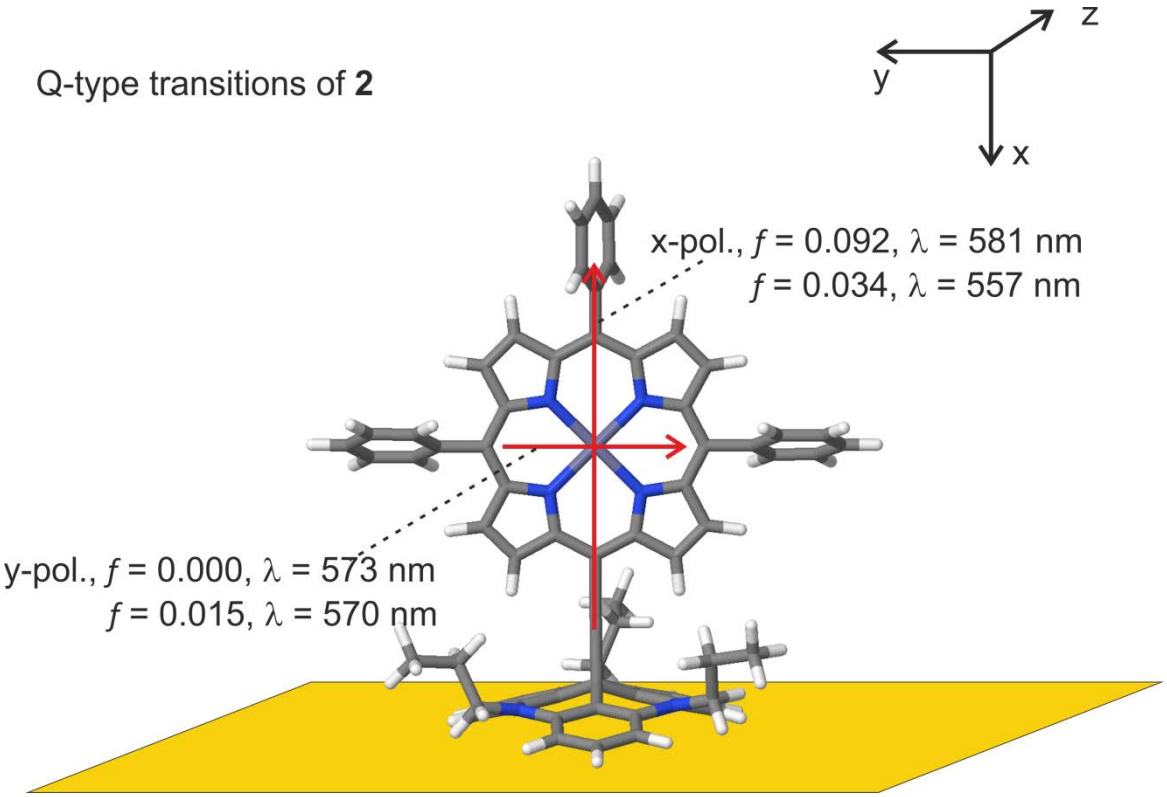

Figure S3 Transition dipole vectors (red arrows), oscillator strengths (*f*), and transition wavelengths (λ/nm) of the Q-type (π-π*) transitions of porphyrin-TATA **2** calculated at the B3LYP/6-31G* level of TDDFT. The four electronic transitions are polarized within the ring plane of the porphyrin (red arrows). Two transitions are x-polarized (perpendicular to the surface, assuming that the molecules stand upright) and two transitions are y-polarized (parallel to the surface). The two x-polarized transitions exhibit medium oscillator strengths (*f*) and the two y-polarized transitions are very weak.

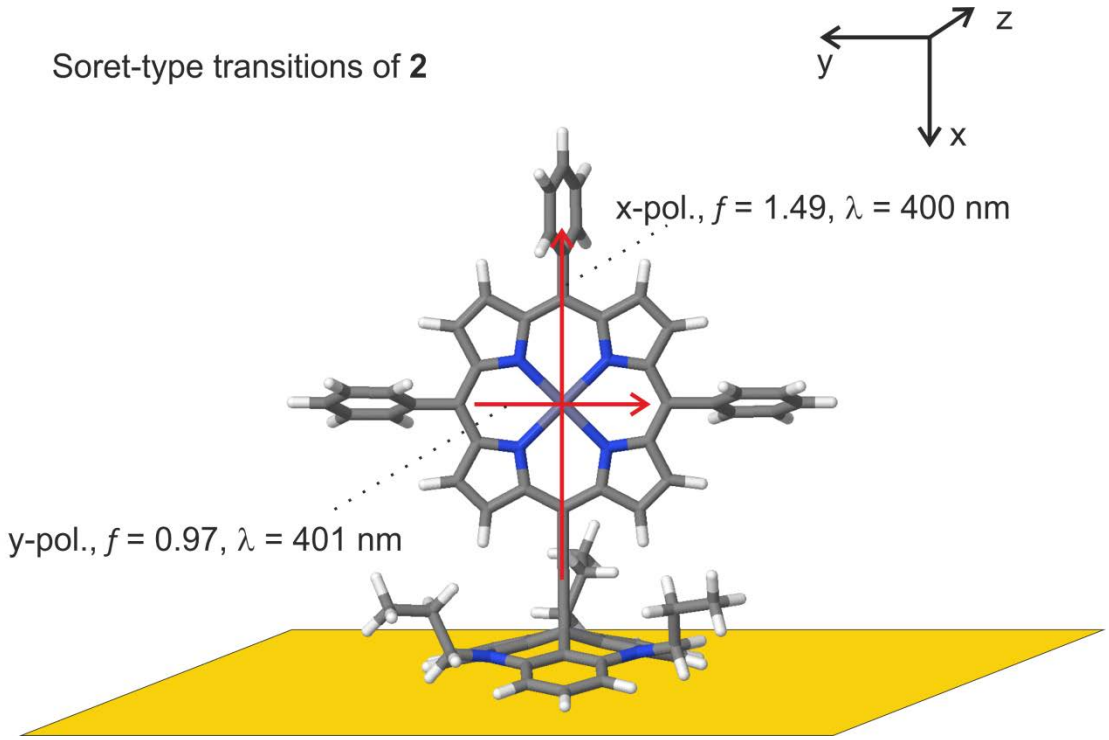

Figure S4 Transition dipole vectors (red arrows), oscillator strengths (*f*), and transition wavelengths (λ/nm) of the Soret-type (π-π*) transitions of porphyrin-TATA **2** calculated at the B3LYP/6-31G* level of TDDFT. The two electronic transitions are polarized within the ring plane of the porphyrin (red arrows) and exhibit extremely large oscillator strengths (*f*=1.49 and 0.97). One transition is x-polarized (perpendicular to the surface, assuming that the molecules stand upright) and one transition is y-polarized (parallel to the surface).

S1.5 Log file excerpt of the TD-DFT calculation of porphyrin-TATA 2

Coordinates:

C	-0.87499	0.47857	-0.84493
C	1.1419	0.0241	0.60554
C	-2.18966	0.13296	-1.33965
N	-0.44923	1.65741	-1.41232
C	-1.45951	2.07574	-2.25889
C	-2.55786	1.12765	-2.2128
N	1.87735	1.13662	0.27031
C	1.86334	-0.78033	1.56843
C	3.05044	1.06882	0.99829
C	3.0468	-0.12892	1.81887
C	-1.4485	3.25493	-3.04419
C	-0.39886	4.20917	-3.06665
C	-0.36467	5.36891	-3.93834
C	0.81418	6.02513	-3.68334
C	1.5042	5.26749	-2.65618
C	4.09285	2.02712	0.97972
C	4.0938	3.21742	0.20824
C	3.50528	4.82561	-1.19831
C	2.78053	5.60242	-2.13734
N	0.74976	4.16695	-2.30335
N	3.09141	3.63014	-0.64589
C	4.80734	5.18489	-0.66851
C	5.178	4.18142	0.19249
H	-2.75367	-0.761	-1.0479
H	-3.4973	1.21721	-2.77104
H	1.50109	-1.72507	1.99191
H	3.84579	-0.42983	2.50658
H	-1.13415	5.63657	-4.67188
H	1.19453	6.93263	-4.16683
H	5.36874	6.09193	-0.92178
H	6.10844	4.10111	0.76663
Zn	1.31616	2.65081	-1.02042
C	-0.14958	-0.30587	0.09999
C	-0.75918	-1.50437	0.57809
C	-1.26968	-2.54977	0.98119
C	1.44955	-6.33174	2.54769
C	0.9386	-6.39309	1.24689
C	-0.19075	-5.60986	0.9064
C	-0.76891	-4.76932	1.88543
C	-0.23698	-4.69972	3.19496
C	0.87737	-5.50954	3.52516
C	-1.88018	-3.81077	1.47599

C	-2.71613	-4.43671	0.36409
C	-4.07165	-4.05587	0.21505
C	-2.09026	-5.28541	-0.58025
C	-2.84278	-5.75963	-1.68249
C	-4.17423	-5.35991	-1.83488
C	-4.79904	-4.51738	-0.90937
C	-2.77153	-3.515	2.67857
C	-2.19057	-3.47477	3.96792
C	-2.97806	-3.07548	5.07407
C	-4.32143	-2.74346	4.8735
C	-4.90885	-2.79489	3.60515
C	-4.13102	-3.17037	2.48226
N	-0.74305	-5.64627	-0.38672
C	0.09884	-6.06106	-1.50975
C	1.25757	-5.08943	-1.79182
N	-4.67108	-3.22719	1.18188
N	-0.83939	-3.83421	4.12826
C	-0.10768	-3.34979	5.29939
C	0.04951	-1.819	5.33259
C	0.81313	-1.34399	6.57146
C	2.10262	-5.52866	-2.99066
C	-5.89511	-2.50342	0.8364
C	-5.67949	-1.39709	-0.21122
C	-6.98049	-0.67408	-0.57067
H	2.31439	-6.96092	2.81574
H	1.40531	-7.06207	0.51167
H	1.2866	-5.52581	4.54462
H	-2.40786	-6.45917	-2.4093
H	-4.75171	-5.73437	-2.6963
H	-5.85169	-4.24315	-1.05636
H	-2.55602	-3.04369	6.08702
H	-4.93977	-2.45151	5.73829
H	-5.97859	-2.56687	3.50699
H	0.4848	-7.09542	-1.35159
H	-0.53725	-6.11113	-2.41292
H	0.82774	-4.07807	-1.9703
H	1.89941	-4.99763	-0.88772
H	-0.58366	-3.71383	6.24081
H	0.90266	-3.79882	5.27793
H	0.57955	-1.49919	4.40716
H	-0.95135	-1.33598	5.29716
H	0.92872	-0.23866	6.56941
H	0.28393	-1.62338	7.51092
H	1.83397	-1.78656	6.61937
H	2.9283	-4.80993	-3.18273

H	2.56271	-6.52934	-2.82343
H	1.49307	-5.5932	-3.92074
H	-6.68583	-3.2135	0.49894
H	-6.28863	-2.03224	1.75492
H	-4.93807	-0.67269	0.19414
H	-5.22276	-1.83229	-1.12762
H	-6.79719	0.13185	-1.31393
H	-7.72879	-1.37163	-1.01103
H	-7.4488	-0.20331	0.32347
C	5.28787	1.76497	1.84532
C	6.17343	0.7037	1.55296
C	5.55651	2.57357	2.97217
C	7.29477	0.45972	2.36166
H	5.9796	0.06992	0.67235
C	6.67643	2.32856	3.78257
H	4.86887	3.40014	3.21472
C	7.5501	1.27115	3.47949
H	7.97758	-0.36955	2.1129
H	6.86491	2.96822	4.66068
H	8.43026	1.07965	4.11515
C	-2.63031	3.51597	-3.9273
C	-2.91603	2.67358	-5.02525
C	-3.48046	4.61976	-3.68931
C	-4.01477	2.92865	-5.86121
H	-2.25531	1.81504	-5.22791
C	-4.58123	4.87326	-4.52278
H	-3.27405	5.28107	-2.83217
C	-4.85146	4.02944	-5.61288
H	-4.21431	2.264	-6.71804
H	-5.23507	5.73694	-4.31681
H	-5.71367	4.23016	-6.27
C	3.4153	6.86634	-2.63202
C	4.57947	6.82896	-3.43184
C	2.85987	8.1259	-2.31365
C	5.17002	8.01381	-3.89838
H	5.01712	5.85268	-3.69714
C	3.45199	9.31114	-2.77733
H	1.95495	8.16974	-1.68592
C	4.60897	9.25941	-3.57183
H	6.07457	7.96224	-4.52697
H	3.00669	10.28434	-2.51169
H	5.07351	10.19018	-3.93729

Electric dipole moments:

Ground to excited state transition electric dipole moments (Au):

state	X	Y	Z	Dip. S.	Osc.
1	-1.3286	0.0052	-0.0569	1.7685	0.0924
2	0.0159	0.0634	0.0123	0.0044	0.0002
3	0.0088	-0.5346	0.0095	0.2860	0.0152
4	-0.7832	-0.0027	0.0487	0.6158	0.0336
5	0.0501	-0.0014	0.0006	0.0025	0.0001
6	-0.0128	0.0122	0.0033	0.0003	0.0000
7	-0.0517	0.0032	-0.0541	0.0056	0.0004
8	-0.0094	-0.0143	0.0009	0.0003	0.0000
9	0.1398	3.5699	0.0342	12.7652	0.9668
10	-4.4278	0.1437	0.0743	19.6318	1.4906

Excitation energies and oscillator strengths:

Excited State 1: Singlet-A 2.1327 eV 581.35 nm f=0.0924 <S**2>=0.000
267 -> 272 -0.22691
270 -> 271 0.66752
This state for optimization and/or second-order correction.
Total Energy, E(TD-HF/TD-KS) = -4785.53070309
Copying the excited state density for this state as the 1-particle RhoCI density.

Excited State 2: Singlet-A 2.1655 eV 572.53 nm f=0.0002 <S**2>=0.000
269 -> 271 0.70445

Excited State 3: Singlet-A 2.1752 eV 569.99 nm f=0.0152 <S**2>=0.000
267 -> 271 0.41739
268 -> 272 0.32754
270 -> 272 0.46456

Excited State 4: Singlet-A 2.2260 eV 556.99 nm f=0.0336 <S**2>=0.000
267 -> 272 -0.32006
268 -> 271 0.61829
270 -> 271 -0.10983

Excited State 5: Singlet-A 2.3392 eV 530.02 nm f=0.0001 <S**2>=0.000
269 -> 272 0.70653

Excited State 6: Singlet-A 2.3496 eV 527.67 nm f=0.0000 <S**2>=0.000
267 -> 271 0.14588
268 -> 272 0.49506

270 -> 272 -0.48249

Excited State 7: Singlet-A 2.6702 eV 464.32 nm f=0.0004 <S**2>=0.000
266 -> 271 0.70387

Excited State 8: Singlet-A 2.8685 eV 432.22 nm f=0.0000 <S**2>=0.000
266 -> 272 0.70688

Excited State 9: Singlet-A 3.0915 eV 401.05 nm f=0.9668 <S**2>=0.000
265 -> 272 0.11923
267 -> 271 0.53785
268 -> 272 -0.37287
270 -> 272 -0.21890

Excited State 10: Singlet-A 3.0992 eV 400.05 nm f=1.4906 <S**2>=0.000
265 -> 271 -0.16806
267 -> 272 0.55634
268 -> 271 0.33002
270 -> 271 0.19101

S1.6 TDDFT calculations of porphyrin-TATA 1

The TDDFT calculation of porphyin-TATA **2** was performed at the B3LYP/6-31G* level of density functional theory. Note that the wavelengths of the transitions predicted by the TDDFT calculations are systematically 10-30 nm hypsochromic with respect to our experimental UV-VIS spectra which is a known problem at this level of theory.[7b] An excerpt of the corresponding log file is given in section S1.7.

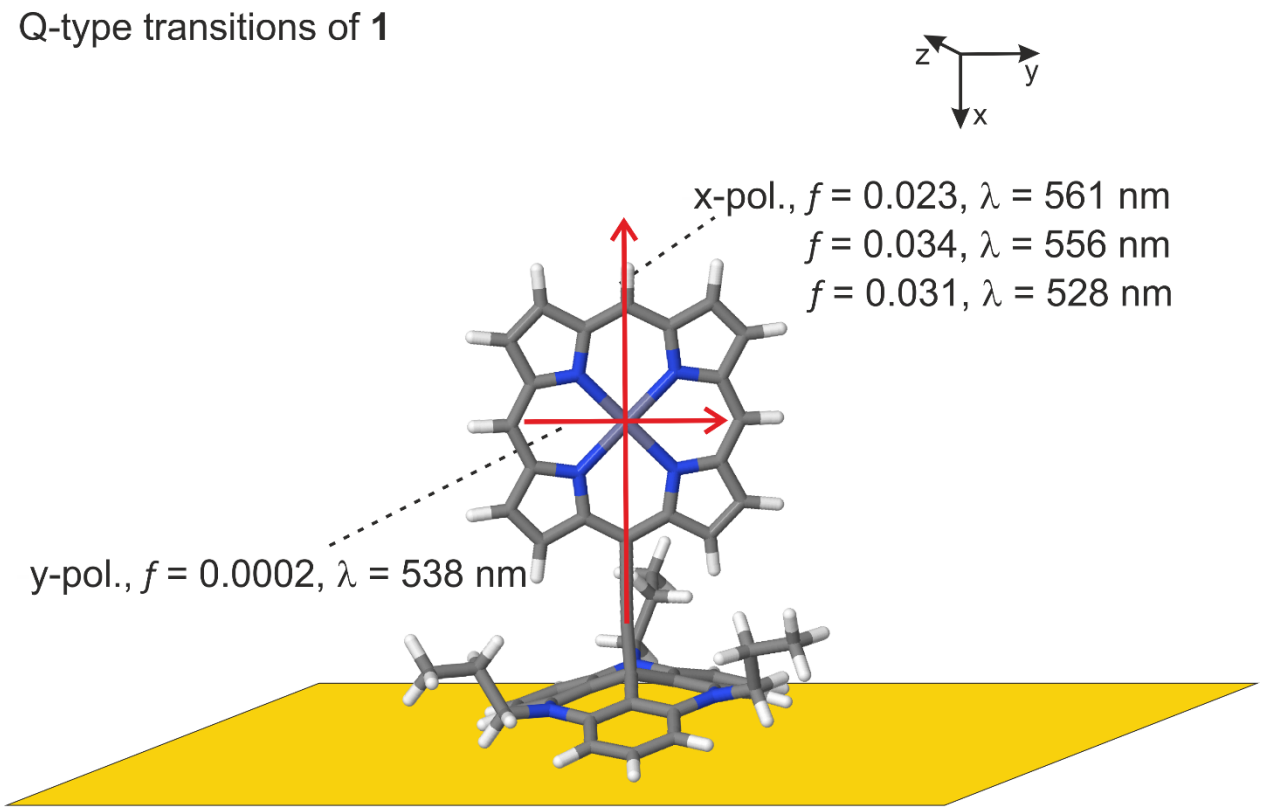

Figure S5 Transition dipole vectors (red arrows), oscillator strengths (*f*), and transition wavelengths (λ/nm) of the Q-type (π-π*) transitions of porphyrin-TATA **1** calculated at the B3LYP/6-31G* level of TDDFT. The four electronic transitions are polarized within the ring plane of the porphyrin (red arrows). Three transitions are x-polarized (perpendicular to the surface, assuming that the molecules stand upright) and one transition is y-polarized (parallel to the surface). The three x-polarized transitions exhibit medium oscillator strengths (*f*) and the y-polarized transition is predicted to exhibit an extremely small extinction.

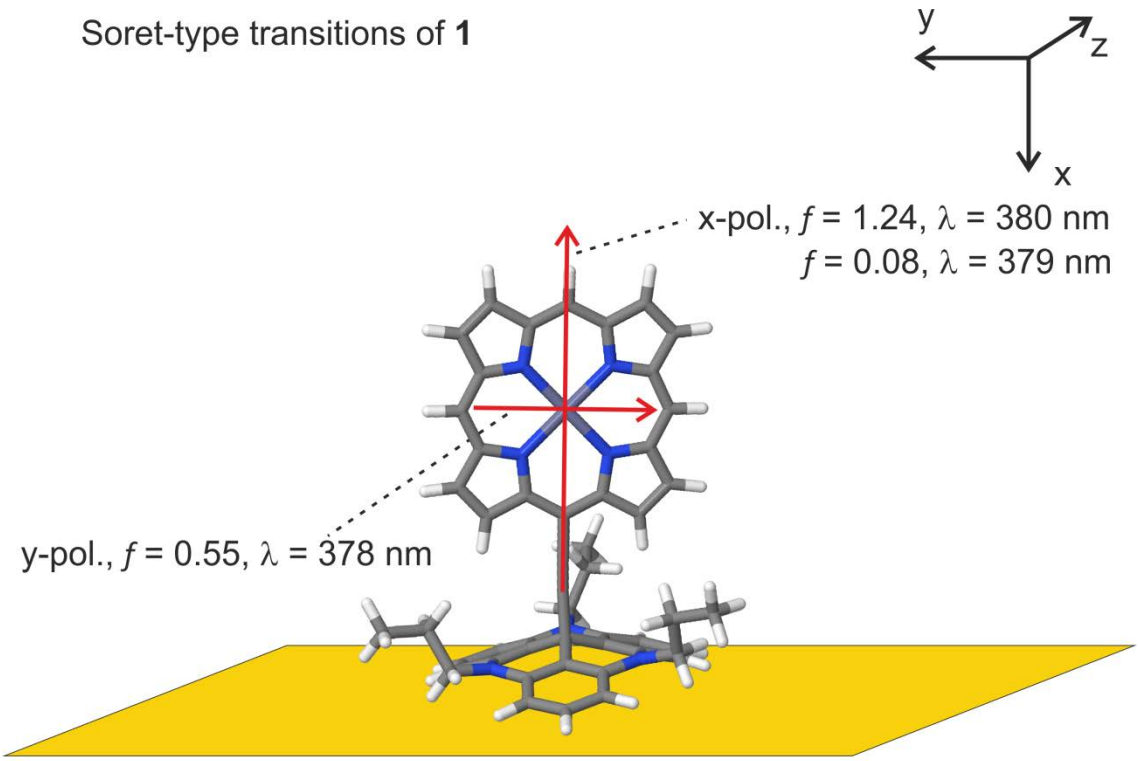

Figure S6 Transition dipole vectors (red arrows), oscillator strengths (*f*), and transition wavelengths (λ/nm) of the Soret-type (π-π*) transitions of porphyrin-TATA **1** calculated at the B3LYP/6-31G* level of TDDFT. The three electronic transitions are polarized within the ring plane of the porphyrin (red arrows). Two transitions are x-polarized (perpendicular to the surface, assuming that the molecules stand upright) and one transition is y-polarized (parallel to the surface).

S1.7 Log file excerpt of the TD-DFT calculation of porphyrin-TATA 1

Coordinates:

C	-0.01771	2.51527	-1.39703
C	2.12293	1.76372	-0.3372
C	-1.4048	2.32469	-1.74918
N	0.43157	3.71398	-1.88835
C	-0.63536	4.29088	-2.54057
C	-1.78605	3.42458	-2.45791
N	2.88464	2.85314	-0.67343
C	2.92039	0.81051	0.39923
C	4.1438	2.61855	-0.1672
C	4.17158	1.34174	0.50323
C	-0.61515	5.52689	-3.18481
C	0.47059	6.39622	-3.29196
C	0.45217	7.67314	-3.96666
C	1.70276	8.20267	-3.84376
C	2.48951	7.25047	-3.09451
C	5.23319	3.48096	-0.27986
C	5.2551	4.72221	-0.91605
C	4.61785	6.50518	-2.03848
C	3.83276	7.40937	-2.75408
N	1.71809	6.16096	-2.76963
N	4.18089	5.29884	-1.5472
C	6.01075	6.6948	-1.70576
C	6.40561	5.58996	-1.0107
H	-1.98913	1.45425	-1.48687
H	-2.75524	3.63822	-2.89121
H	2.55922	-0.13811	0.77107
H	5.04139	0.91324	0.98548
H	-1.54306	5.8457	-3.6515
H	-0.40947	8.09901	-4.46557
H	2.0694	9.14876	-4.22222
H	6.16216	3.15061	0.17663
H	4.31572	8.32612	-3.08043
H	6.59987	7.56283	-1.97444
H	7.38239	5.37294	-0.59654
Zn	2.30357	4.51053	-1.7165
C	0.75576	1.59109	-0.65793
C	0.11952	0.39668	-0.20513
C	-0.40255	-0.62385	0.19928
C	2.37112	-4.4447	1.57891
C	1.78525	-4.49388	0.31862
C	0.66298	-3.69132	0.04862
C	0.15994	-2.84564	1.05103

C	0.76618	-2.79406	2.31795
C	1.87438	-3.61939	2.5827
C	-0.98099	-1.88969	0.71895
C	-1.88638	-2.52823	-0.32756
C	-3.24925	-2.18676	-0.36776
C	-1.3336	-3.38785	-1.29275
C	-2.16105	-3.91139	-2.30232
C	-3.50247	-3.54849	-2.34628
C	-4.05932	-2.69797	-1.3973
C	-1.78784	-1.61389	1.9836
C	-1.13023	-1.58781	3.22534
C	-1.84511	-1.23449	4.38253
C	-3.19978	-0.93977	4.28183
C	-3.86674	-0.98446	3.06219
C	-3.15661	-1.30565	1.89108
N	0.03219	-3.7155	-1.2072
C	0.78466	-4.14797	-2.38784
C	1.97573	-3.23321	-2.71612
N	-3.77638	-1.34154	0.62624
N	0.23382	-1.92435	3.28702
C	1.05146	-1.43236	4.39884
C	1.17693	0.09947	4.42695
C	2.04038	0.57719	5.59875
C	2.71959	-3.69901	-3.97176
C	-5.04255	-0.64739	0.38251
C	-4.96378	0.38747	-0.75148
C	-6.3161	1.06482	-0.99614
H	3.2244	-5.08312	1.7927
H	2.18486	-5.16089	-0.43522
H	2.32817	-3.64736	3.56579
H	-1.77887	-4.61889	-3.02777
H	-4.1371	-3.95978	-3.12693
H	-5.11346	-2.45699	-1.44867
H	-1.36039	-1.21283	5.35063
H	-3.75786	-0.69171	5.18088
H	-4.93334	-0.80033	3.03982
H	1.11652	-5.19077	-2.28025
H	0.10395	-4.12953	-3.23822
H	1.5976	-2.21295	-2.85391
H	2.66645	-3.19671	-1.86716
H	0.6698	-1.80617	5.35982
H	2.05119	-1.85023	4.28473
H	1.61305	0.42856	3.47567
H	0.18322	0.55602	4.48714
H	2.13162	1.6685	5.59828

H	1.60809	0.28091	6.56283
H	3.05397	0.15995	5.54821
H	3.55922	-3.03369	-4.19914
H	3.12347	-4.71155	-3.84625
H	2.05997	-3.712	-4.84843
H	-5.85102	-1.36799	0.19201
H	-5.31433	-0.11775	1.29393
H	-4.21056	1.13716	-0.47907
H	-4.61443	-0.08937	-1.67347
H	-6.24317	1.81134	-1.79421
H	-7.08071	0.33615	-1.29311
H	-6.67811	1.57654	-0.09573

Electric dipole moments:

Ground to excited state transition electric dipole moments (Au):

state	X	Y	Z	Dip. S.	Osc.
1	-0.6502	0.0534	-0.0370	0.4270	0.0231
2	0.2429	0.0186	0.0453	0.0614	0.0034
3	0.0120	0.0601	0.0031	0.0038	0.0002
4	-0.7283	-0.0051	0.0360	0.5317	0.0306
5	-0.0478	0.0765	0.0028	0.0082	0.0005
6	-0.0062	-0.1215	-0.0009	0.0148	0.0009
7	-0.0327	0.0062	-0.0507	0.0037	0.0002
8	0.0161	0.0024	-0.0025	0.0003	0.0000
9	3.9170	0.3666	-0.0144	15.4779	1.2373
10	1.0237	-0.0148	-0.0057	1.0482	0.0839
11	-0.6853	2.5282	0.0211	6.8618	0.5515

Excitation energies and oscillator strengths:

Excited State 1: Singlet-A 2.2119 eV 560.53 nm f=0.0231 <S**2>=0.000
207 ->212 0.10376
209 ->211 0.11186
210 ->211 0.68857
This state for optimization and/or second-order correction.
Total Energy, E(TD-HF/TD-KS) = -4092.39292027
Copying the excited state density for this state as the 1-particle RhoCI density.

Excited State 2: Singlet-A 2.2318 eV 555.52 nm f=0.0034 <S**2>=0.000
209 ->211 0.69567
210 ->211 -0.10670

Excited State 3: Singlet-A 2.3043 eV 538.05 nm f=0.0002 <S**2>=0.000
207 ->211 0.44119
208 ->212 -0.40597
210 ->212 -0.36780

Excited State 4: Singlet-A 2.3462 eV 528.44 nm f=0.0306 <S**2>=0.000
207 ->212 0.41195
208 ->211 0.56655

Excited State 5: Singlet-A 2.4112 eV 514.19 nm f=0.0005 <S**2>=0.000
207 ->211 0.10589
208 ->212 -0.17734
209 ->212 0.54339
210 ->212 0.40154

Excited State 6: Singlet-A 2.4243 eV 511.43 nm f=0.0009 <S**2>=0.000
207 ->211 -0.15853
208 ->212 0.28228
209 ->212 0.44818
210 ->212 -0.43980

Excited State 7: Singlet-A 2.7343 eV 453.44 nm f=0.0002 <S**2>=0.000
206 ->211 0.70421

Excited State 8: Singlet-A 2.9428 eV 421.32 nm f=0.0000 <S**2>=0.000
206 ->212 0.70688

Excited State 9: Singlet-A 3.2630 eV 379.96 nm f=1.2373 <S**2>=0.000
204 ->211 -0.17003
205 ->211 0.24418
207 ->212 0.49097
208 ->211 -0.37883

Excited State 10: Singlet-A 3.2681 eV 379.38 nm f=0.0839 <S**2>=0.000
204 ->211 0.68277
207 ->212 0.12666

Excited State 11: Singlet-A 3.2806 eV 377.93 nm f=0.5515 <S**2>=0.000
205 ->212 -0.20236
207 ->211 0.48438
208 ->212 0.44013

S2 Experimental Section

S2.1 STM details

STM images were obtained under ambient conditions using a PicoPlus STM (Agilent) and mechanically cut PtIr tips. Typically, a tunneling current I_t in the range 7 to 15 pA and a tunneling bias of 0.3 to 0.8 V was used. The displayed images were mildly filtered to reduce noise.

High resolution images of the porphyrin-TATA adlayer (Figure S7) reveal a triangular shape of the molecules, in which three equidistant maxima in each molecule are clearly resolved. Similar images have been obtained previously for TATA derivatives with other vertical groups (phenyl, azobenzene) and can be attributed to the three benzene rings of the TATA platform. Because of the small barrier for in-plane rotation of the vertical group and the sufficiently large TATA-TATA spacing, the orientation of these groups will change rapidly on the time-scale of the STM imaging at room temperature. For this reason, these groups only provide an overall uniform contribution and the contrast in the submolecular resolution is dominated by the static TATA unit. Such observation of atomic or molecular features underneath highly mobile species is a well-known effect in high resolution STM. The small variations in contrast between different molecules and between the three maxima within each molecule, respectively, may originate from local hindering of the rotation by the alkyl side chains as well as direct contributions of the side chains to the image. Furthermore, for these open adlayers physisorption of airborne contaminations from the surrounding environment in between the vertical groups cannot be rigorously excluded for images obtained under ambient conditions.

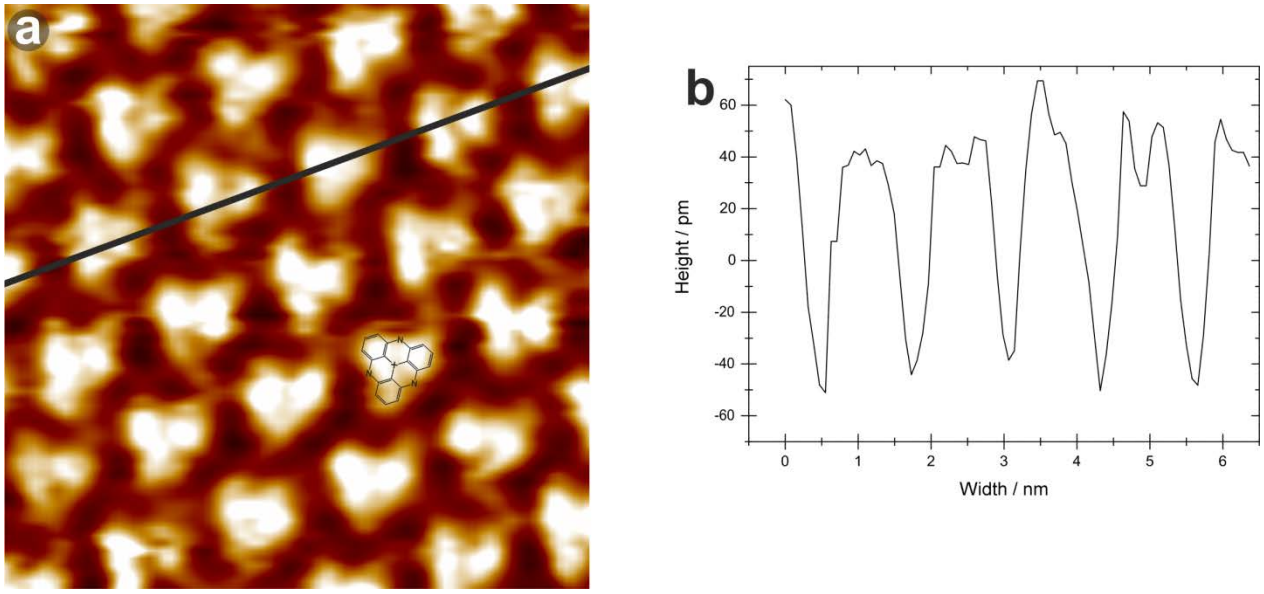

Figure S7 (a) High-resolution STM image of porphyrin-TATA adlayers of 1 (6×6 nm², I_t= 9 pA, U_{Bias}=0.5 V) and (b) cross section along the line shown in the image. To indicate the orientation of the TATA platform a to-scale model is overlaid on one of the molecules visible in (a). (b) Cross section along the black line shown in the image in (a).

To better illustrate the double row structure of the adlayer, the average apparent height in the STM images along the direction normal to the double rows is shown in Figure S8. The characteristic structure consisting of double rows with a weak minimum in between (≈ 20 pm modulation), separated by deeper minima (≈ 80 pm modulation) is clearly visible.

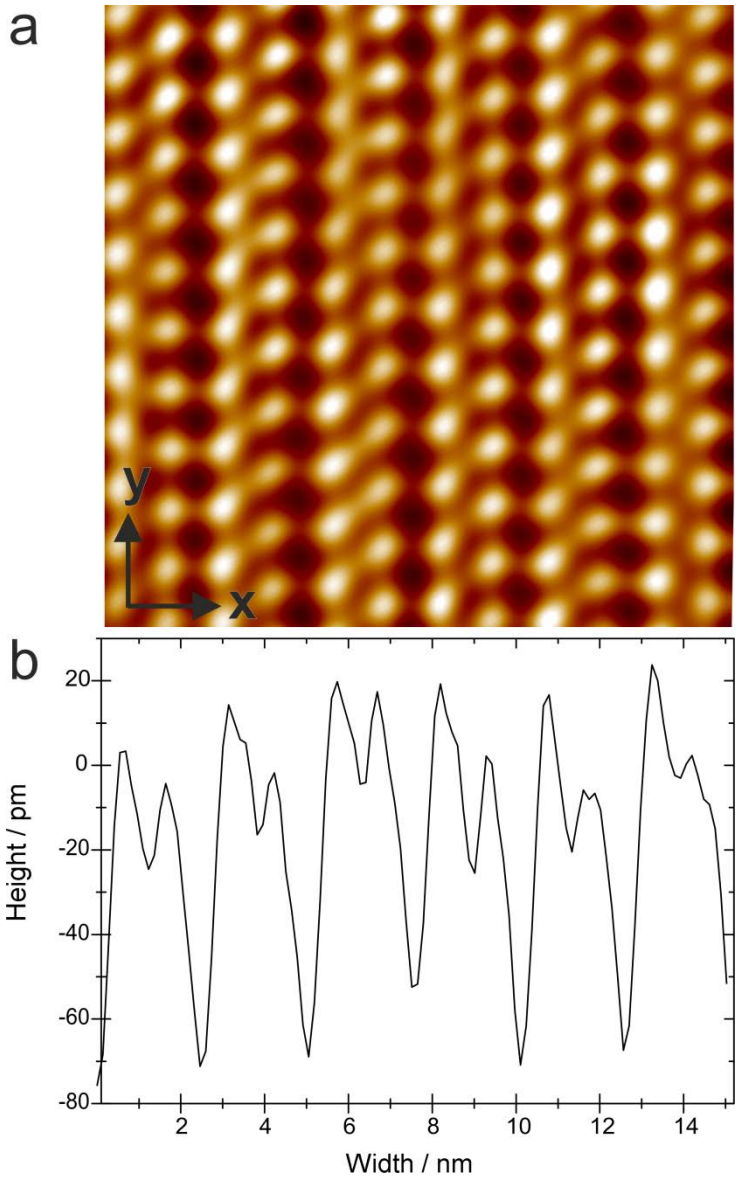

Figure S8 (a) High-resolution STM image of porphyrin-TATA adlayers of **2** (14.8 × 15.0 nm², I_t= 13 pA, U_{Bias}= 0.48 V) and (b) average height distribution normal to the molecular rows, obtained by averaging over the entire y range of the image in (a). The unfiltered original STM data was used to obtain the data in (b).

S2.2 Synthetic procedures

5-Trimethylsilylethinylporphin

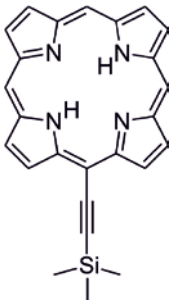

2,2'-Dipyrromethane (500 mg, 3.42 mmol) was dissolved under nitrogen in dry chloroform (225 mL) and formalin (37 wt % in water) (339 µL, 3.42 mmol) and 3-trimethylsilyl-2-propynale (251 µL, 1.71 mmol) was added. Then, $BF_3{\cdot}O(Et)_2$ (94.0 µL, 762 mmol) was injected, and the solution was stirred at RT for 1h. After that, *p*-chloranil (450 mg, 183 mmol) was added under air, and the mixture was allowed to stir for another 1 h. The solvent was removed in vacuo, and the solid was purified by chromatography on silica gel (0.043-0.060), first using dichlormethane, and then twice with dichloromethane:*n*-hexane 5:2 as eluent (R_f = 0.76). The product was obtained as a purple solid (50.0 mg, 123 µmol, 7 %).

^{1}H-NMR (500 MHz, $CDCl_3$): δ = 10.2 (s, 2H), 10.1 (s, 1H), 9.81 (d, ^3J = 4.5 Hz, 2H), 9.33 (d, ^3J = 4.5 Hz, 2H), 9.31 (s, 4H), 0.67 (s, 9H), -2.81 (br s, 2H). **^{13}C-NMR** (125.8 MHz, $CDCl_3$): δ = 148.9, 140.7, 131.4, 131.3, 130.6, 106.6, 105.5, 105.3, 101.9, 98.5, 0.43.

MS (EI, 70 eV): m/z (%) = 406 (100) $[M]^+$, **MS** (CI, Isobutan): m/z (%) = 407 (100) $[M+H]^+$.

Anal. calcd. for $C_{25}H_{22}N_4Si$ (406.16) C 73.86, H 5.45, N 13.78, Found: C 73.96, H 5.74, N 13.60; UV-Vis (CH_2Cl_2) λ_{max} (lg ε): 413 (5.13), 507 (3.75), 542 (3.74), 581 (3.33), 637 (3.26) nm; m.p.>400° C.

(5-Trimethylsilylethinylporphyrinato)-zinc(II)

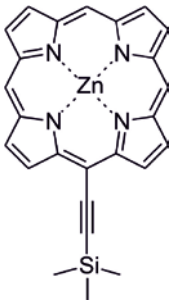

5-Trimethylsilylethinylporphyrine (50.0 mg, 123 µmol) was dissolved in chloroform (30 mL), then zinc acetate dihydrate (200 mg, 911 µmol) dissolved in methanol (10 ml) was added and the mixture was stirred at RT for 20 h. The mixture was washed with water, the layers were separated, and the organic layer was dried with Na_2SO_4.

The solvent was removed in vacuo, and the residue purified by chromatography on silica gel (0.043-0.060) using dichloromethane as eluent. The product was obtained as a purple solid (57.0 mg, 123 µmol, >98%).

^{1}H-NMR (500 MHz, $CDCl_3$): δ = 10.16 (s, 2H), 10.1 (s, 1H), 9.86 (d, ^{3}J = 4.3 Hz, 2H), 9.42-9.39 (m, 6H), 0.69 (s, 9H). **^{13}C-NMR** (125.8 MHz, $CDCl_3$): δ = 139.2, 132.9, 132.1, 107.6, 0.40. **MS** (EI): m/z (%) = 468 (100) $[M]^+$, **MS** (CI): m/z (%) = 469 (100) $[M+H]^+$.

Anal. calcd. For $C_{25}H_{20}N_4SiZn$ (468.07) C 63.90, H 4.29, N 11.92, found C 63.67, H 4.95, N 11.83; UV-Vis (CH_2Cl_2) λ_{max} (lg ε): 413 (5.36), 545 (4.06), 583 (3.84) nm; m.p.>400° C.

5-Trimethylsilyethinyl-10,15,20-triphenylporphyrine and (**5-Trimethylsilylethinyl-10,20-diphenyl porphyrinato) Zn(II)** were prepared according to a procedure by Fathalla et al.[8] For alternative methods see ref 9-11.

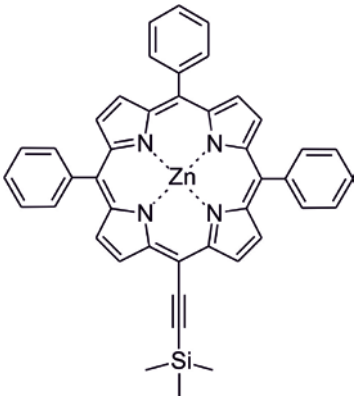

(5-Trimethylsilyethinyl-10,15,20-triphenylporphyrinato)-manganese(III) chloride

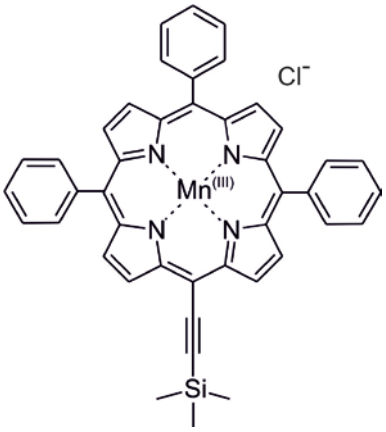

5-Trimethylsilylethinyl-10,15,20-triphenylporphyrin (20.0 mg, 31.5 µmol) was dissolved in dry dimethylformamide (200 ml) and refluxed under nitrogen. Manganese chloride tetrahydrate (200 mg, 1.11 mmol) was added and refluxed for a further period of 2 h.

Water (400 ml) was added, and the solution was stirred for a further period of 12 h. Dichloromethane was added to the reaction mixture, the phases were separated, and the organic layer was dried with Na_2SO_4 and filtered. The solvent was removed in vacuo. The product was purified on a short column of basic aluminum oxide using chloroform and methanol as eluent. The product was obtained as a green solid (9.00 mg 12.5 µmol, 40 %).

MS (ESI): m/z (%) = 687.1 (100) $[M\text{-}Cl]^+$; Anal. calcd. for $C_{43}H_{32}N_4SiMnCl$ (722.15) C 71.41, H 4.46, N 7.75, found C 71.67, H 3.95, N 7.83; UV-Vis (CH_2Cl_2) λ_{max} (lg ε): 380 (4.17), 408 (4.12), 483 (4.95), 591 (3.67), 636 (3.62) nm; m.p.>400° C.

General method to prepare porphyrine functionalized TATA platforms:[12-15]

Powdered KOH (in excess) was added to a solution of trimethylsilylethynyl substituted porphyrins in 40 mL THF under nitrogen. The mixture was sonicated for 40 min at RT using a Branson Sonifier W-450. After adding 4,8,12-tri-*n*-octyl-4,8,12-triazatriangulenium tetrafluoroborate (1 equiv.), the mixture was sonicated for a period of 4–6.5h at 10-15 °C. The mixture was poured into 100 mL of a concentrated NaCl solution. The layers were separated and the aqueous layer was extracted with diethyl ether. The combined organic layers were dried with $NaSO_4$ and filtered. After evaporating the solvents, the residue was first dissolved in diethylether, and filtered through a short column of basic aluminum oxide and the solvent was evaporated. The residue was dissolved in ethylacetate:*n*-hexane (1:1), and filtered through a short column of basic aluminum oxide. The solvent was evaporated, and the product was obtained in pure form.

{5-[(4,8,12-Tri-*n*-octyl-4,8,12-triazatriangulene-12c-yl)-ethinyl]-porphyrinato}-zinc(II) 1

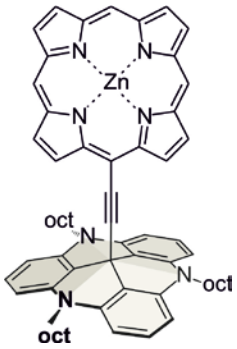

Following the general method (above), KOH (500 mg, 8.91 mmol) was added to a solution of (5-trimethylsilylethinylporphyrinato)-zinc(II) (60.0 mg, 127 µmol) in 40 mL THF. After 30 min of sonication, 4,8,12-tri-*n*-octyl-4,8,12-triazatriangulenium tetrafluoroborate (89.5 mg, 127 µmol) was added, and the mixture was sonicated for 4 h. The red product was obtained in a yield of 42 % (55.0 mg, 54.0 µmol).

^{1}H-NMR (600 MHz, $CDCl_3$): δ = 9.87 (s, 1H), 9.40 (s, 2H), 9.20 (d, ^3J = 4.1 Hz, 2H), 9.09 (d, ^3J = 4.1 Hz, 2H), 8.70 (d, ^3J = 4.1 Hz, 2H), 8.60 (d, ^3J = 4.1 Hz, 2H), 7.46 (t, ^3J = 8.3 Hz, 3H), 6.87 (d, ^3J = 8.3 Hz, 6H), 4.27 (t, ^3J = 8.3 Hz, 6H), 2.12-2.06 (m, 6H), 1.62-1.56 (m, 6H), 1.41-1.36 (m, 6H), 1.23-1.18 (m, 6H), 1.14-1.07 (m, 12H), 0.71 (t, ^3J = 6.9 Hz, 9H);

^{13}C-NMR (150 MHz, $CDCl_3$): δ = 150.3, 148.3, 147.6, 147.1, 140.9, 131.7, 131.5, 130.7, 130.4 128.7, 110.0, 106.0, 105.2, 105.1, 100.1, 98.7, 85.6, 46.9, 31.7, 29.7, 29.4, 29.3, 27.2, 26.0, 22.6, 13.9; **MS** (ESI, 649-2000): m/z (%) = 1014.5 (100) $[M+H]^+$, 1013.6 (13) $[M]^+$; **MS** (ESI): m/z (%) = 1014.5 (4) $[M+H]^+$, 618.3 (100) $[M-C_{22}H_{12}N_4Zn]^+$;

Anal. calcd. for $C_{65}H_{71}N_7Zn$ (1015.69) C 76.86, H 7.05, N 9.65, found C 75.98, H 6.88, N 9.23; UV-Vis (C_7H_8): λ_{max} (lg ε) = 326 (4.44), 422 (5.35), 551 (4.27), 586 (4.04) nm; m.p.>400° C.

{5-[(4,8,12-Tri-*n*-octyl-4,8,12-triazatriangulene-12c-yl)-ethinyl]-10,15,20-triphenyl-porphyrinato}-zinc(II) 2

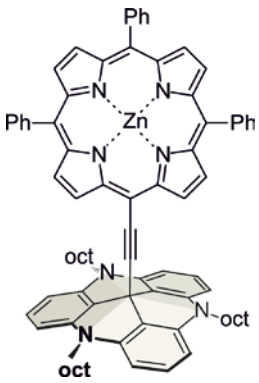

Following the general method described above, KOH (556 mg, 9.91 mmol) was added to a solution of (5-trimethylsilylethinyl-10,15,20-triphenylporphyrinato)-zinc(II) (74.2 mg, 106 µmol) in 40 mL THF. After 30 min of sonication, 4,8,12-tri-n-octyl-4,8,12-triazatriangulenium tetrafluoroborate (75.0 mg, 100 µmol) was added and the mixture was sonicated for 6.5 h. The blue greenish product was obtained in a yield of 72 % (95.4 mg (76.7 µmol).

^{1}H-NMR (500 MHz, $CDCl_3$): δ = 9.15 (d, ^3J = 4.6 Hz, 2H), 8.80 (d, ^3J = 4.6 Hz, 2H), 8.76 (d, ^3J = 4.6 Hz, 2H), 8.15-8.11 (m, 6H, H-2-Ph, H-6-Ph), 7.77-7.68 (m, 9H), 7.30 (t, ^3J = 8.3 Hz, 3H), 6.70 (d, ^3J = 8.3 Hz, 6H), 4.07 (t, ^3J = 8.3 Hz, 6H), 1.99-1.92 (m, 6H), 1.49-1.45 (m, 6H), 1.30-1.26 (m, 6H), 1.15-1.12 (m, 6H), 1.06-1.01 (m, 12H), 0.68 (t, ^3J = 6.9 Hz, 9H) ppm.

^{13}C-NMR (125 MHz, $CDCl_3$): δ = 150.2, 149.8, 140.7, 134.3, 132.2, 131.9, 131.6, 131.4, 128.5, 127.4, 126.5, 122.0, 121.4, 110.2, 105.0, 100.5, 90.1, 80.1, 46.7, 31.7, 29.7, 29.3, 29.2, 27.1, 26.0, 22.6, 14.2; **MS** (ESI, 651-2000): m/z (%) = 1244.6 (95) [M+H], 1243.6 (100) $[M]^+$; **MS** (ESI): m/z (%) = 1243.6 (4) $[M]^+$, 618.3 (100) $[M-C_{39}H_{26}N_4Zn]^+$;

Anal. calcd. for $C_{83}H_{83}N_7Zn$ (1243.97) C 80.14, H 6.72, N 7.88, found C 79.06, H 6.77, N 7.23; UV-Vis (CH_3CN): λ_{max} (lg ε) = 273 (4.59), 293 (4.54), 326 (4.31), 433 (5.30), 570 (4.00), 616 (4.12) nm; m.p.>400°C.

{5-[(4,8,12-Tri-n-octyl-4,8,12-triazatriangulene-12c-yl)-ethinyl]-10,20-diphenyl-porphyrinato}-zinc(II)

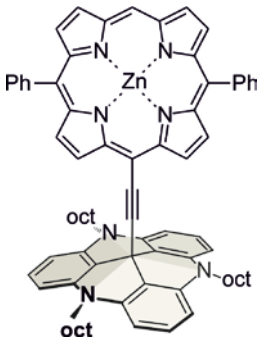

Following the general method described above, KOH (350 mg, 6.24 mmol) was added to a solution of (diphenyl-10-dimethylsilylethinylporphyrinato)-zinc(II) (43.9 mg, 70.6 µmol) in 40 mL THF. After 30 min of sonication, 4,8,12-tri-*n*-octyl-4,8,12-triazatriangulenium tetrafluoroborate (52.0 mg, 73.7 µmol) was added and the mixture was sonicated for 5 h. The product was obtained as a red solid in a yield of 11 % (9.00 mg, 7.72 µmol).

^{1}H-NMR (500 MHz, CDCl 3): δ = 10.1 (s, 1H), 9.23 (d, ^{3}J = 4.6 Hz, 2H), 9.17 (d,^{3}J = 4.6 Hz, 2H), 8.91 (d, ^{3}J = 4.6 Hz, 2H), 8.77 (d, ^{3}J = 4.6 Hz, 2H), 8.13-8.09 (m, 4H), 7.78-7.72 (m, 6H), 7.30 (t, ^{3}J = 8.3 Hz, 3H), 6.69 (d, ^{3}J = 8.3 Hz, 6H), 4.07 (t, ^{3}J = 8.3 Hz, 6H), 1.98-1.93 (m, 6H), 1.48-1.45 (m, 6H), 1.29-1.25 (m, 6H), 1.15-1.12 (m, 6H), 1.07-1.01 (m, 12H), 0.67 (t, ^{3}J = 6.9 Hz, 9H) ppm. ^{13}C-NMR (125 MHz, CDCl 3): δ = 151.6, 150.0, 149.4, 149.3, 142.5, 140.7, 134.3, 132.1, 131.9, 131.5, 131.2, 128.5, 127.3, 126.5, 122.6, 110.1, 106.8, 105.0, 100.6, 98.1, 80.1, 46.8, 31.7, 29.8, 29.4, 29.3, 27.1, 26.0, 22.7, 14.0; **MS** (ESI, 699-1500): m/z (%) = 1167.6 (98) $[M+H]^{+}$, 1166.6 (100) $[M]^{+}$; **MS** (ESI): m/z (%) = 1167.6 (3) $[M+2]^{+}$, 1166.6 (4) $[M]^{+}$, 618.3 (100) $[M\text{-}C_{34}H_{20}N_4Zn]^{+}$.

Anal. calcd. for $C_{77}H_{79}N_7Zn$ (1167.88) C 79.19, H 6.82, N 8.40, found C 79.69, H 6.84, N 8.70 %; UV-Vis (CH_3CN): λ_{max} (lg ε) = 273 (4.12), 292 (4.03), 324 (3.87), 428 (4.87), 564 (3.63), 608 (3.54) nm; m.p.>400°C.

{5-[(4,8,12-Tri-n-octyl-4,8,12-triazatriangulen-12c-yl)-ethinyl]-10,15,20-triphenyl-porphyrinato}-manganese(III) chloride

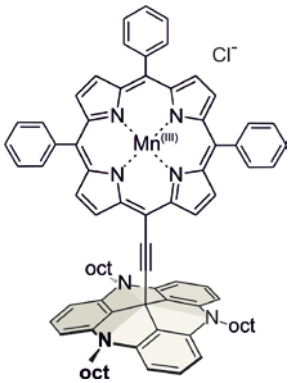

Following the general method described obove, KOH (50 mg, 89.1 µmol) was added to a solution of (5-trimethylsilylethinyl-10,15,20-triphenylporphyrinato)-manganese(III)chlorid (9.00 mg, 12.5 µmol) in 40 mL THF. After 30 min of sonication, 4,8,12-Tri-n-octyl-4,8,12-triazatrianguleniumtetrafluoro-borate (15.0 mg, 21.2 µmol) was added and the mixture was sonicated for 5 h. The red product was obtained in a yield of 40 % (6.50 mg, 5.13 µmol), mp.: > 400 °C.

MS (ESI, 1220-1250): m/z (%) = 1233.6 (92) $[M\text{-}Cl+H]^+$, 1232.6 (100) $[M\text{-}Cl]^+$; **MS** (ESI): m/z (%) = 1233.6 (12) $[M\text{-}Cl+H]^+$, 1232.6 (13) $[M\text{-}Cl]^+$, 618.5 (100) $[M\text{-}C_{39}H_{26}N_4MnCl]^+$; Anal. calcd. for $C_{83}H_{83}N_7MnCl$ (1267.55) C 78.56, H 6.59, N 7.73, found C 79.96, H 6.37, N 8.43 %; UV-Vis ($CH_3COOC_2H_5$): λ_{max} (lg ε) = 335 (4.28), 377 (4.40), 406 (4.35), 480 (4.68), 598 (3.67), 640 (3.88) nm.

References:

(1) TURBOMOLE V6.2 2010, a development of University of Karlsruhe and Forschungszentrum Karlsruhe GmbH, TURBOMOLE GmbH, since 2007; available from http://www.turbomole.com., 1989-2007.

(2) A. D. Becke, *J. Chem. Phys.* **1993**, *98*, 5648-5652.

(3) C. Lee, W. Yang, R.G. Parr, *Phys. Rev. B* **1988**, *37*, 785-789.

(4) P. J. Stephens, F. J. Devlin, C. F. Chabalowski, M. J. Frisch, *J.Phys.Chem.* **1994**, *98*, 11623-11627.

(5) Gaussian 09, Revision **D.01**, M. J. Frisch, G. W. Trucks, H. B. Schlegel, G. E. Scuseria, M. A. Robb, J. R. Cheeseman, G. Scalmani, V. Barone, B. Mennucci, G. A. Petersson, H. Nakatsuji, M. Caricato, X. Li, H. P. Hratchian, A. F. Izmaylov, J. Bloino, G. Zheng, J. L. Sonnenberg, M. Hada, M. Ehara, K. Toyota, R. Fukuda, J. Hasegawa, M. Ishida, T. Nakajima, Y. Honda, O. Kitao, H. Nakai, T. Vreven, J. A. Montgomery, Jr., J. E. Peralta, F. Ogliaro, M. Bearpark, J. J. Heyd, E. Brothers, K. N. Kudin, V. N. Staroverov, R. Kobayashi, J. Normand, K. Raghavachari, A. Rendell, J. C. Burant, S. S. Iyengar, J. Tomasi, M. Cossi, N. Rega, J. M. Millam, M. Klene, J. E. Knox, J. B. Cross, V. Bakken, C. Adamo, J. Jaramillo, R. Gomperts, R. E. Stratmann, O. Yazyev, A. J. Austin, R. Cammi, C. Pomelli, J. W. Ochterski, R. L. Martin, K. Morokuma, V. G. Zakrzewski, G. A. Voth, P. Salvador, J. J. Dannenberg, S. Dapprich, A. D. Daniels, Ö. Farkas, J. B. Foresman, J. V. Ortiz, J. Cioslowski, and D. J. Fox, Gaussian, Inc., Wallingford CT, 2009.

(6) N. Hauptmann, K. Scheil, T.G. Gopakumar, F. L. Otte, C. Schütt, R. Herges and R. Berndt, *J. Am. Chem. Soc.* **2013** , *135*, 8814-8817.

(7) a) S. Grimme, J. Antony, S. Ehrlich and H. Krieg, *J. Chem. Phys*. **2010** ,132, 154104; b) S. Grimme, M. Parac, *ChemPhysChem* **2003**, *4*, 292.

(8) M. Fathalla, J. Jayawickramarajah, *Eur. J. Org. Chem.* **2009**, *35*, 6095-6099.

(9) S. Achelle; N. Saettel, P. Baldeck, M.-P. Teulade-Fichou, P. Maillard, *J. Porph. Phthal.* **2010**, *14*, 877-894.

(10) F. Hammerer, G. Garcia, S. Chen, F. Poyer, S. Achelle, C. Fiorini-Debuisschert, M.-P. Teulade-Fichou, P. Maillard, *J. Org. Chem.* **2014** , *79*, 1406 – 1417.

(11) A. Ryan, A. Gehrold, R. Perusitti, M. Pintea, M. Fazekas, O. B. Locos, F. Blaikie, O. M. Senge, *Eur. J. Org. Chem.* **2011**, *29*, 5817-5844.

(12) D. R. B. Baisch, U. Jung, O. M. Magnussen, C. Nicolas, J. Lacour, J. Kubitschke, R. Herges, *J. Am. Chem. Soc.* **2009**, *131*, 442-443.

(13) J. Kubitschke, C. Näther, R. Herges, *Eur. J. Org. Chem.* **2010**, 5041-5055.

(14) S. Kuhn, B. Baisch, U. Jung, T. Johannsen, J. Kubitschke, R. Herges, O. Magnussen, *Phys. Chem. Chem. Phys.* **2010**, *12*, 4481-4487.

(15) W. Laursen, F. C. Krebs, *Chem. Eur. J.* **2001**, *7*, 1773-1783.